

- ✓ Tin liquid limiter experiments
- ✓ Post-disruption Runaway Electron beam mitigation
- ✓ Tearing mode studies with MARS code
- ✓ Highly collisional regimes
- ✓ Diagnostics
 - Runaway Electron Imaging Spectroscopy for in-flight RE
 - Triple Cherenkov probe for escaping RE
 - Laser Induced Breakdown Spectroscopy
 - Collective Thomson Scattering
 - Dust studies with infrared camera

Tin liquid limiter experiments (1)

❑ The Tin Liquid Limiter was tested with standard FTU pulses ($B_T = 5.3$ T, $I_p = 0.5$ MA). The maximum thermal load deduced by the Langmuir probes was about 15 MW/m² for almost 1 s, without any degradation of the plasma performance, proving liquid tin to be a good candidate as a Plasma Facing Components material.

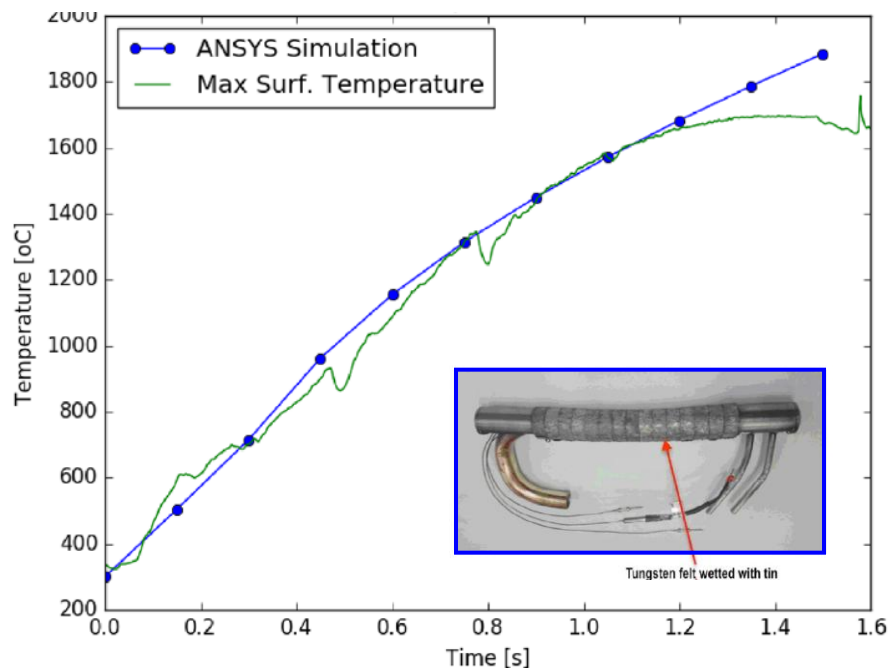
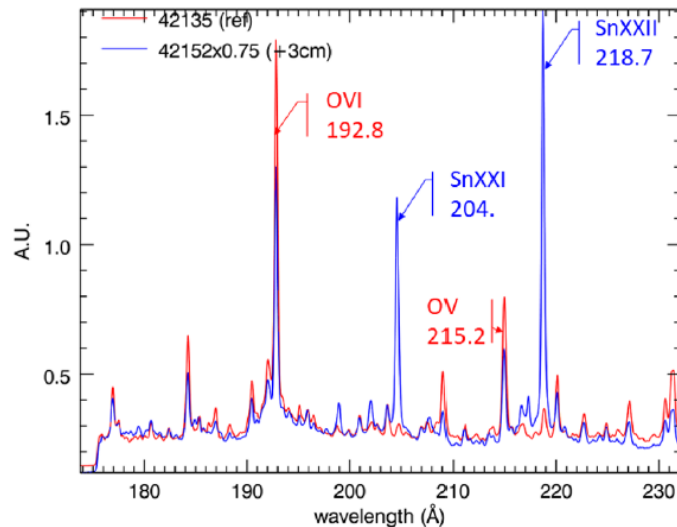


Figure 1. Experimental surface temperature (recorded with a fast Infrared camera) compared with the ANSYS model. The flattening of the surface temperature can be linked to the evaporation phenomena.

| | |
|---------------|-----------------------|
| Mazzitelli G. | IAEA FIP/3-5Rb (2018) |
| Iafrati M. | EPS O5.132 (2017) |
| Apruzzese G. | EPS P4.1025 (2018) |

Tin liquid limiter experiments (2)



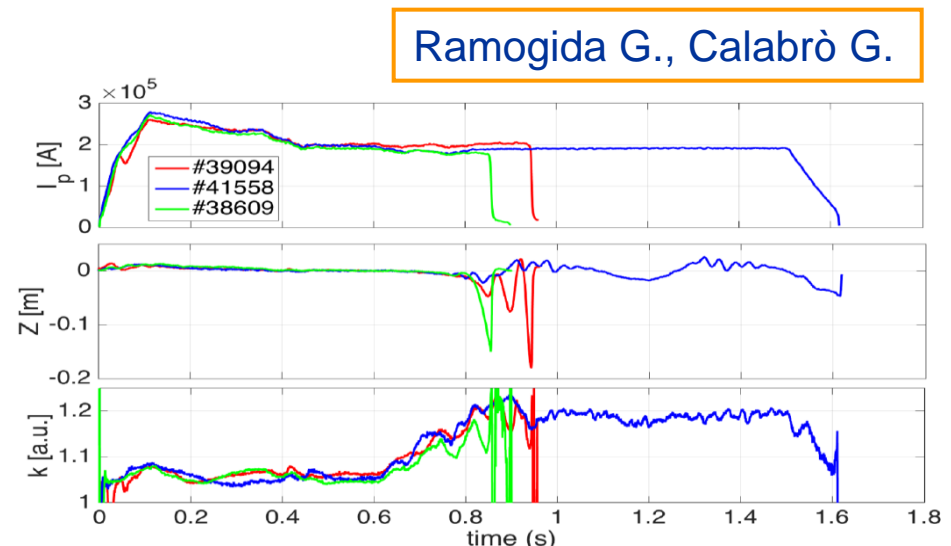
□ A 2 m grazing incidence **Schwob-Fraenkel XUV spectrometer** was installed on FTU observing the plasma emission in the range from 20 to 340 Å, to identify the spectral lines of Sn, with high spectral resolution

Figure 2. Comparison of one segment of the spectrum observed by the Schwob-Fraenkel XUV spectrometer for two discharges, one with the TLL fully retracted (in red), and the other with the TLL at +3 cm (in blue).

Bombarda F. EPS P1.1005 (2018)

□ A new vertical controller has been designed to stabilize **vertically elongated plasmas in FTU**, where VDEs have been observed. Experimental results showed its capability of stabilizing plasma up to the FTU record elongation of 1.23.

Figure 3. Comparison between the standard PID controller (red and green lines) and the new hybrid (continuous and discrete) controller (blue lines).



Post-disruption RE beam mitigation

□ Stabilization and suppression of post-disruption RE beam has been achieved on FTU, with a control architecture that allows to detect the current quench and to induce via the central solenoid a controlled RE beam current ramp-down meanwhile the beam is kept away from the vessel.

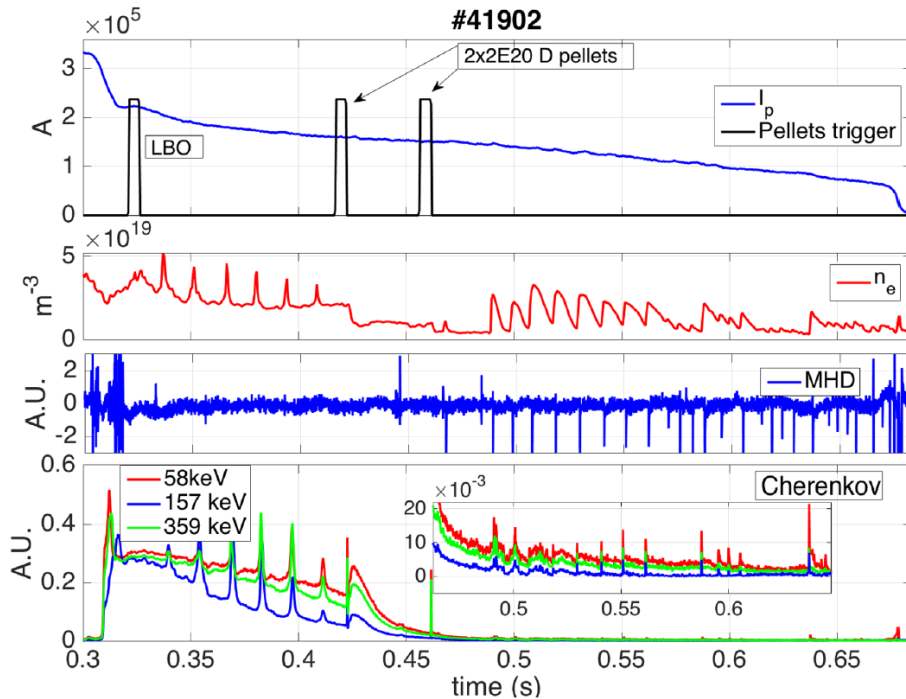
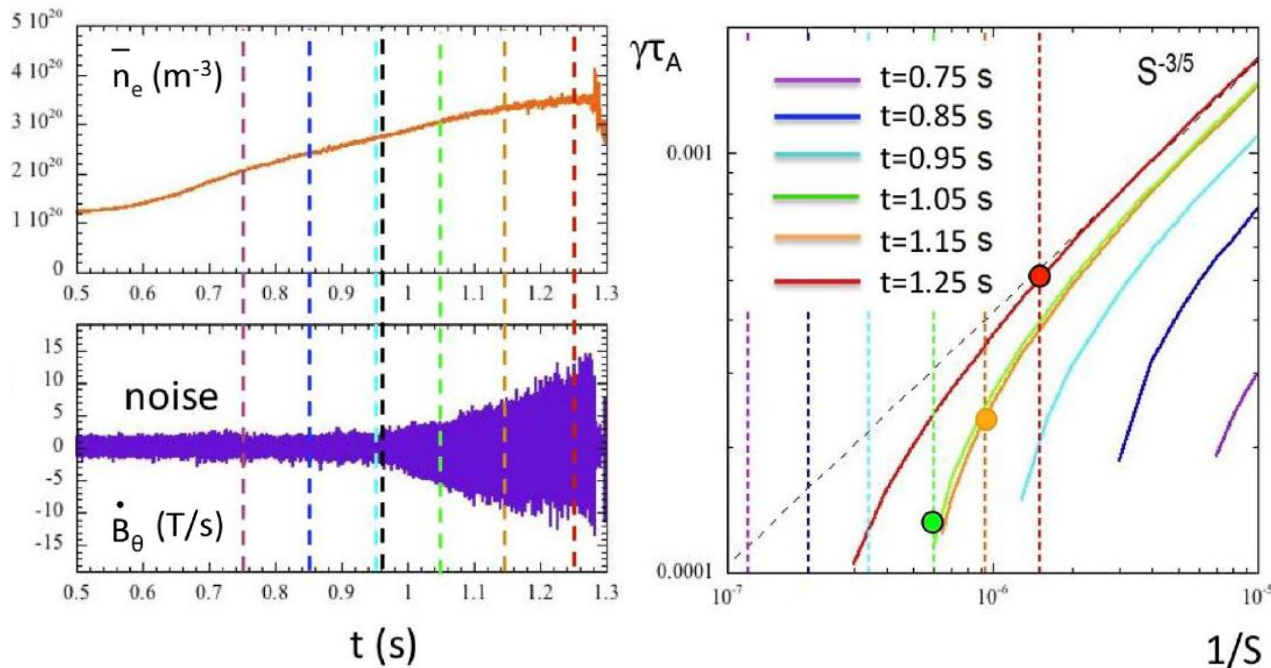


Figure 4. Iron LBO and D pellet injections on a post-disruption RE beam. Cherenkov probe spikes reveal that runaways are expelled from the beam core due to plasma instabilities. The origin of the RE expulsions after the iron injection is under investigation, whereas a sequence of fan-like instability events seems to take place after D pellet injections.

Carnevale D. PPCF 61 (2019)
Romano A. EPS P5.1053 (2018)

Tearing mode studies with MARS code

□ The onset of TMs in the high-density regime has been analyzed by means of the MARS code, which is a global, resistive, spectral code for full MHD linear stability analysis. The obtained onset times have been compared with the ones observed experimentally from pick-up coil signals and a good agreement can be claimed.



Fusco V., Vlad G.

Figure 5. FTU pulse #34769. $B_T=8\text{T}$, $I_p=0.9\text{MA}$. (Left) Line-averaged central density and perturbed poloidal magnetic field evolution. (Right) MARS output for different times (equilibria) during the density ramp-up. The effective values of the experimental inverse Lundquist number in FTU are shown as vertical dotted lines.

□ An increase of the density peaking with the effective collisionality ν_{eff} has been found on FTU at very high values of ν_{eff} . This behavior seems to be related to an edge phenomenon, as the MARFE instability presence and ameliorated conditioning of wall by using the Li limiter

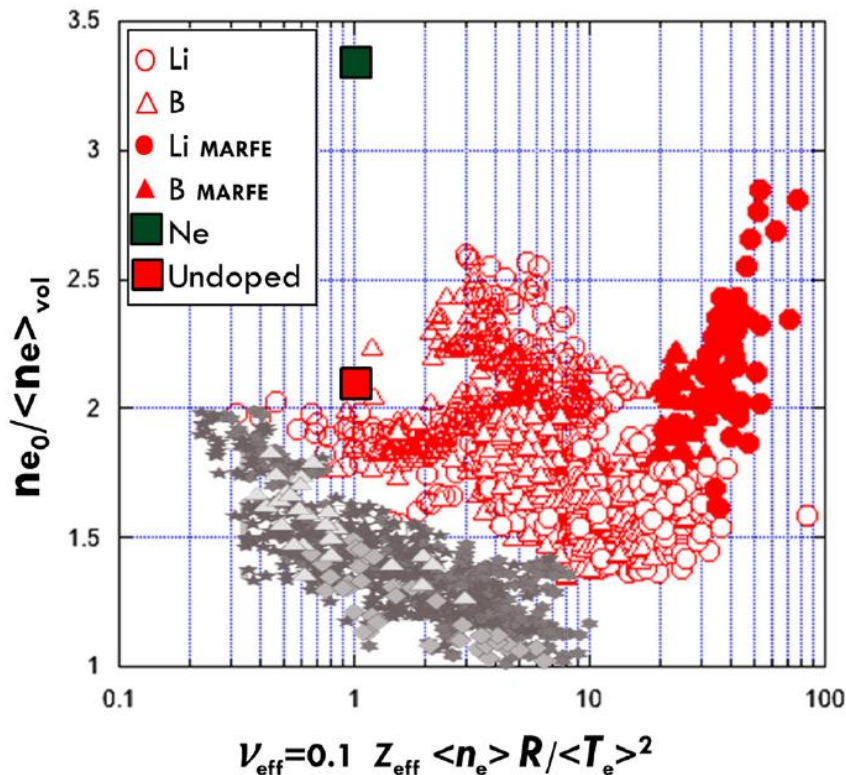
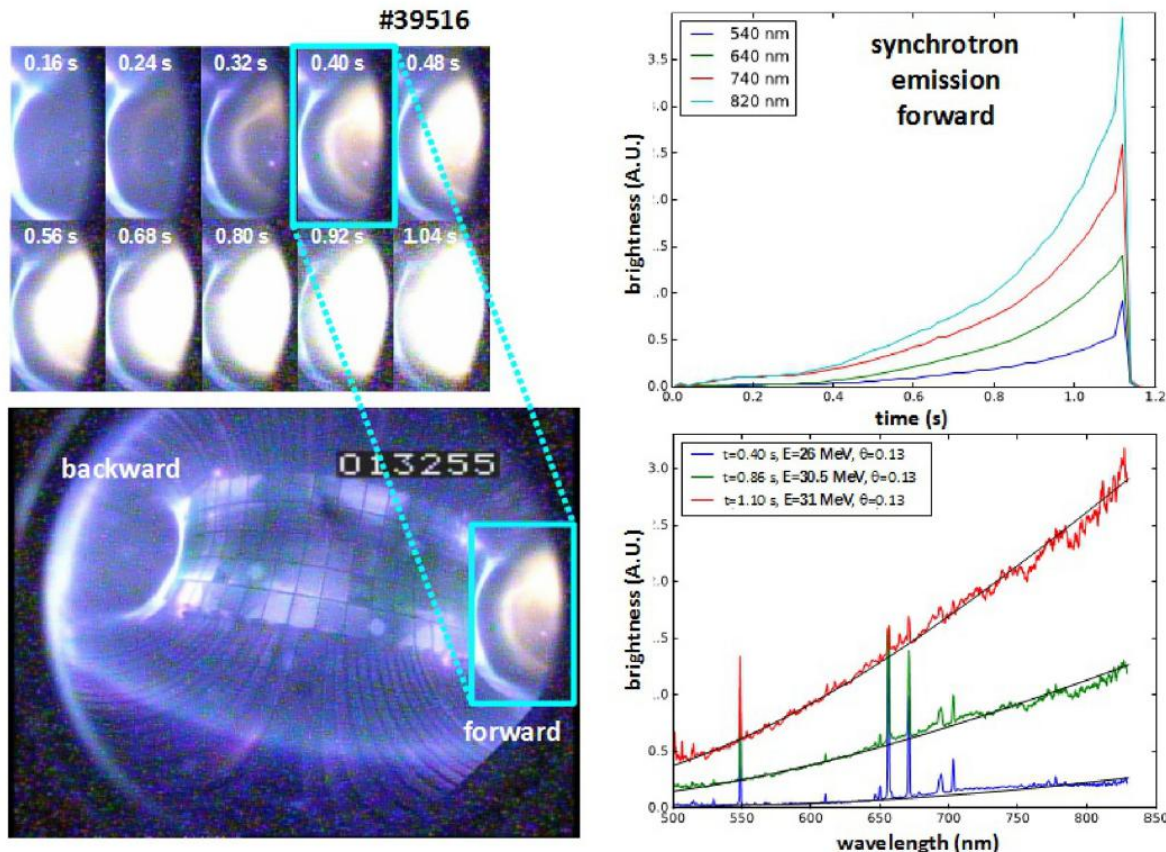


Figure 6. Density peaking as a function of the effective collisionality. Red symbols for FTU data; grey symbols for other devices. The behavior of a neon doped pulse on FTU is also reported.

Mazzotta C. EPS P2.179 (2017)



□ The REIS diagnostic has allowed to provide simultaneously the image and the visible/infrared spectrum of the forward and backward radiation from in flight REs.

Esposito B. PPCF **59** (2017)

Figure 7. Pulse #39516. (Left) Visible camera images of the RE beam: the bottom image shows both RE backward and forward views at $t = 0.4$ s, while the top image is a time sequence of the forward view. (Right) Measured synchrotron radiation intensity at several wavelengths (top) and synchrotron radiation spectra (bottom), fitted assuming mono-energetic distributions.

Triple Cherenkov probe

❑ A triple Cherenkov probe was installed and tested on FTU, confirming the Cherenkov probe to be a valid diagnostic system to study and monitor plasma scenarios involving REs.

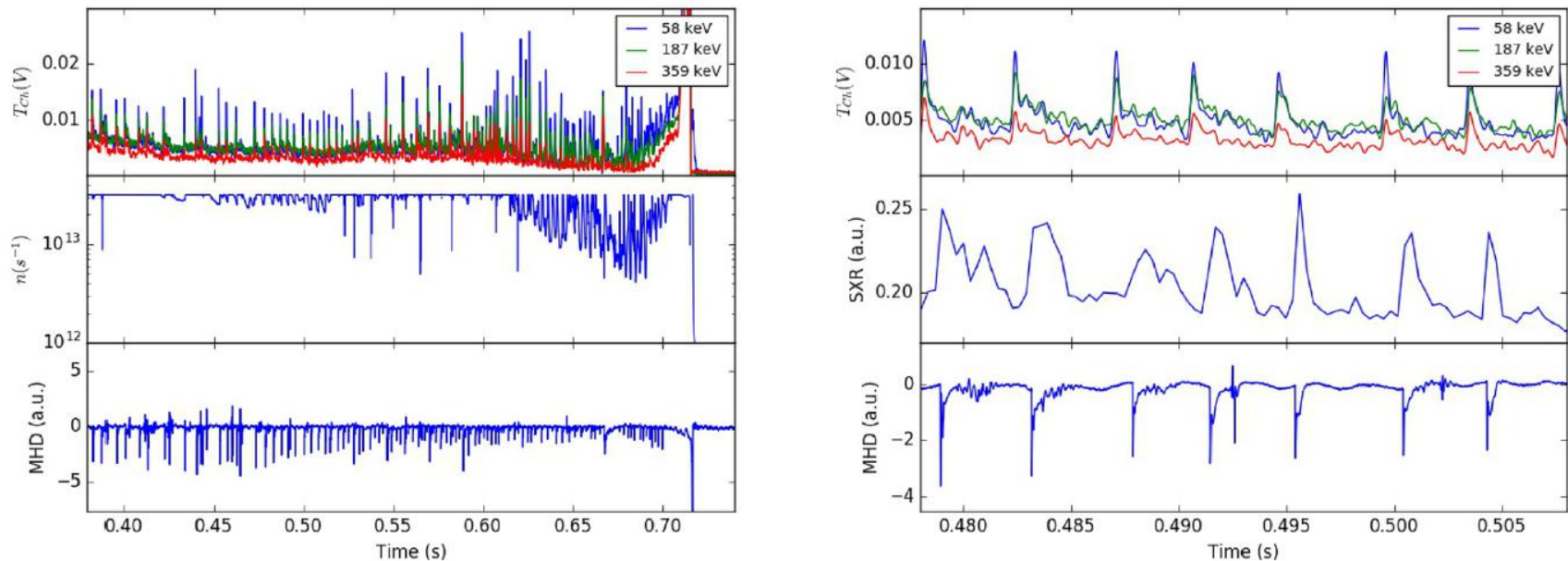


Figure 8. (Left) Correlation between triple Cherenkov probe signal, gamma-ray count rate and MHD activity. (Right) Triple Cherenkov signal, soft x-rays and MHD activity. Pulse #41146.

Bagnato F. PPCF 60 (2018)

❑ **Laser Induced Breakdown Spectroscopy** measurements of the deuterium retained on the FTU Mo toroidal limiter tiles have shown that LIBS is a suitable not invasive in situ diagnostic for a quantitative detection of tritium retained in the ITER vessel components.

Maddaluno G., Almaviva S.

❑ The CTS diagnostics was used for investigations on **Parametric Decay Instability** excitation by EC beams in correlation with magnetic islands induced by neon injection. Parasitic emissions from the gyrotron were observed, while other spectral emissions have been observed and analyzed.

Baiocchi B. EPS P4.1015 (2018)

❑ Recent investigation on FTU proved the presence of **Dust mobilized** prior to pulse start-up phase, when in the tokamak volume the magnetic field consists just of the time growing toroidal and multipole components due to the external coils.

De Angeli M.